Scientia Horticulturae 368 (2026) 115219

Contents lists available at ScienceDirect

Scientia Horticulturae

journal homepage: www.elsevier.com/locate/scihorti

Research Paper

Soil moisture and vapour pressure deficit predict trunk water potential in field-grown kiwifruit

Giuseppe Montanaro, Maria Calabritto *, Alba Nicoletta Mininni, Bartolomeo Dichio

Università Degli Studi della Basilicata, Agricultural, Forestry, Food and Environmental Science Department, Viale dell'Ateneo Lucano 10, Potenza, 85100, Italy

ARTICLE INFO

Keywords:
Capacitance
Hydraulic resistance
Irrigation
Model
Plant-based sensor
Soil water content
Stomatal conductance
VPD

ABSTRACT

A dynamic model has been developed to predict trunk water potential (Ψ_{trunk}) from soil water content (*SWC*) and air vapour pressure deficit (*VPD*) in field-grown kiwifruit. The model included a capacitor (trunk tissue) apart of soil in order to account for the time lag between transpiration and Ψ_{trunk}. Sub-models were defined from known, calibrated or specifically developed relationships linking *SWC* or *VPD* to hydraulic resistances of the whole soil-leaf path and of the storage compartment, plant leaf area and transpiration. Estimation of soil water potential from *SWC* was also included. The estimations of Ψ_{trunk} (Ψ_{model}) were compared with *in vivo* measurements via microtensiometers installed in vines under full irrigation or progressively droughted. The resulting Ψ_{model} values were closely related to actual ones showing a median R^2 up to approx. 0.95. The model revealed that the daily water released by the compartment to the transpiration stream (up to 0.22 m^3 ha^{-1}) makes the orchard almost entirely dependent on root water uptake, posing a significant challenge for irrigation management. The main advantage of the model proposed is the limited number (two) of operational inputs variables supporting the employment of a combination of model and sensors to enable easy, and relatively low-cost monitoring of plant water status and in turn irrigation management.

1. Introduction

Nowadays there is an increasing interest in soil and plant-based sensors for continuous and real-time measuring of those traits shaping plant response to the surrounding environment and management (e.g., soil moisture, sap flow, temperature, stem and leaf water potential) (Scalisi et al., 2017; Noun et al., 2022; Restrepo-Acevedo et al., 2026). The resulting information ecosystem would support the transition of agriculture towards the digital domain improving the efficiency in using natural resources (e.g., water, soil) and crop adaptation to climate changes (Ali et al., 2025; Parra-López et al., 2025).

Advantages and pitfalls of plant-based sensors for irrigation management purpose (i.e., dendrometry, fruit gauges, and other tissue water content sensors, growth, sap flow, stomatal conductance) have been reviewed (Jones, 2004) envisaging their pivotal role in precision irrigation. Recently, "plant wearable" sensors along with remote sensing platforms (e.g., UAV) and imaging (e.g., RGB) for water status monitoring come to the forum (Carella et al., 2024; Velazquez-Chavez et al., 2024; Wu S. et al., 2025). However, certain plant-based sensors might be invasive and potentially cause physical damage to the plant (e.g., Di Biase et al., 2025; Wu N. et al., 2025), and possibly require accurate calibration and data management for reliability (Green et al., 2003; Fernández, 2014; Villalobos et al., 2025). These limitations are likely hampering large scale adoption of such sensors and drawing attention to non-invasive or even contactless sensors (Walsh et al., 2024; Park et al., 2025). Within this context modelling plant response might further assist in data-driven agriculture.

In their review Velazquez-Chavez et al. (2024) showed that stem water potential and trunk diameter changes are among the most used parameters for monitoring plant water status or irrigation management. However, implementing a 1:1 sensor/plant would be challenging in real world. Hence, a trade-off between plant-based sensors accuracy and practical deployment at field scale is desirable. Again, modelling of the plant response could be supportive in gain a wide range of information based on relatively low number of probes.

Stem water potential (Ψ_{trunk}) is a plant physiological trait that aggregates the response of plant to both environmental (e.g., soil moisture, radiation, vapour pressure deficit) and management features (e.g., irrigation, pruning) as mediated by leaf functioning (e.g., stomatal conductance and transpiration) (McCutchan and Shackel, 1992; Naor,

* Corresponding author.
E-mail address: maria.calabritto@unibas.it (M. Calabritto).

https://doi.org/10.1016/j.scienta.2026.115219
Received 30 December 2025; Received in revised form 1 October 2026; Accepted 5 October 2026
Available online 12 October 2026
0304-4238/© 2026 The Authors. Published by Elsevier B.V. This is an open access article under the CC BY-NC license (http://creativecommons.org/licenses/by-nc/4.0/).

1998; Fereres and Goldhamer, 2003; Shackel, 2011; Haberstroh et al., 2025). Such response is also mediated by internal factors (e.g., phenological stage, leaf area, fruit load) (Marsal and Girona, 1997; Girona et al., 2004) including the hydraulic resistance and capacitance of the water transport pathway (Scholz et al., 2007, 2011; Meinzer et al., 2009; Calabritto et al., 2025). Taking all this together, the drop in water potential from soil to leaf is proportional to (*i*) the overall resistance across the soil-plant-atmosphere path and (*ii*) leaf transpiration (Van den Honert, 1948; Scharwies and Dinneny, 2019).

Transpiration rate is intimately related to vapor pressure deficit (*VPD*) because of the tight response of stomatal conductance (g_s) to *VPD*. Although the underlying mechanisms of the dependence of g_s to *VPD* remain debated (Grossiord et al., 2020), the stomatal aperture in response to *VPD* variation has been modelled (Oren et al., 1999). Hence, variations of Ψ_{trunk} would be consistent to those in g_s as estimated through the g_s:*VPD* relationship (Oren et al., 1999; Meinzer, 2003; Grossiord et al., 2020).

The overall resistance across the soil-plant-atmosphere path is also regulated by soil water content (*SWC*). As soil dries, a root-soil air gap is created because of the root shrinkage decreasing soil hydraulic conductivity and in turn increasing the overall soil-plant resistance (Nobel, 2005). In line with this, the influence of *SWC* on the hydraulic resistance along the plant transport pathway has been documented in various tree species including kiwifruit (Baert et al., 2015; Salomón et al., 2017; Calabritto et al., 2025).

Due to the causation effect of *VPD* and *SWC* on Ψ_{trunk}, several studies aimed at modeling the Ψ_{trunk} measured through microtensiometer focusing the response of the sensor to *VPD* and *SWC* even within additive linear models (Pagay, 2022; Blanco and Kalcsits, 2021; 2023; Haberstroh et al., 2025; Vaccaro et al., 2025). However, in those models a large variability in the prediction remains likely because models were developed under a steady-state condition rather than dynamic accounting for the hysteresis between *VPD* and Ψ_{trunk} by shifting backward the Ψ_{trunk} series (Blanco and Kalcsits, 2021; Di Biase et al., 2025).

Hence, a Ψ_{trunk} model should account for the time lag between maximum transpiration (underlying the peak in *VPD*) and the minimum Ψ_{trunk} employing the capacitance effect of the trunk to supply water to balance the transpiration stream (Calkin and Nobel, 1986, Meinzer et al., 2004; Nobel, 2005; Haberstroh et al., 2025). In line with this, leaf and trunk capacitors are often included in dynamic (non-steady-state) models (Calkin and Nobel, 1986; Tyree, 1988; Steppe et al., 2006, Paschalis et al., 2024). Inclusion of capacitors is relevant for estimations at diurnal time scale of transpiration and absorption fluxes while it would have no effect on daily totals (Hunt et al., 1991; Paschalis et al., 2024). Recently, measurements of trunk sap flow and Ψ_{trunk} were used in combination with a dynamic water flow model to estimate hydraulic capacitance (C) and hydraulic resistance (R) in kiwifruit (Calabritto et al., 2025). However, predictions of Ψ_{trunk} employing C, R and easily accessible environmental factors (i.e., *SWC, VPD*) remain challenging. Modelling Ψ_{trunk} would be supportive in minimize certain barriers due to difficulties in its large-scale deployment (e.g., total number of sensors per ha).

On this background, the present study aimed to develop a dynamic model of diurnal Ψ_{trunk} based on *VPD* and *SWC* data leveraging previous efforts defining plant internal factors (e.g., hydraulic resistances) (Calabritto et al., 2025).

2. Materials and methods

2.1. Site description and treatments imposition

The study was conducted in a mature yellow-fleshed kiwifruit vineyard (*A. chinensis* var. *chinensis* cv. 'Zesy002') located in Southern Italy (Metaponto, 40°24′N 16°46′E). The vines were grafted on D1 rootstock (*A. chinensis* var. *deliciosa*) with a 5 × 2 m vine spacing (1000 vines ha^{-1}) and trained to pergola system. Full details on the site are reported in Di Biase et al. (2025). Briefly, soil field capacity was 39.48% vol. and wilting point was 18.49% vol. Vines were irrigated by a single micro-sprinkler per vine (40 L h^{-1} discharging rate) wetting a soil zone of 0.90 m radius. Irrigation volumes were determined daily based on reference evapotranspiration. Two irrigation levels were imposed. Fully irrigated vines received about 60 m^3 ha^{-1} day^{-1} and served as control (CTRL). Starting from a week after the beginning of the experiment (August), a group of vines were progressively subjected to drought receiving 0-15 m^3 ha^{-1} day^{-1}. However, to avoid the occurrence of an abrupt stress, after the initial three days of water restriction, about 35 m^3 H_2O ha^{-1} were supplied a day for two days. The experiment lasted for about 30 days.

Air temperature and relative humidity were recorded hourly by a standard weather station (SKU-6253, Davis Instruments, USA) installed in the vineyard and connected to a wireless data-logger system (Winet S. r.l. Cesena, Italy). Hourly air vapor pressure deficit (*VPD*, kPa) was then calculated (Goudriaan and van Laar, 1994).

Soil volumetric water content (*SWC*, % vol.) was continuously monitored using a 90 cm Frequency Domain Reflectometry (FDR) multi-profile soil moisture probe (SENS-STk90 Drill & Drop, Sentek Sensor Technologies Stepney, Australia). This study focused on *SWC* changes in the 0–30 cm soil depth, which has been reported to be primarily affected by vine water uptake (Calabritto et al., 2024). The *SWC* probes (one per treatment) were positioned on the row close to adjacent vines (two vines per treatment) equipped with microtensiometers (FloraPulse, Davis, CA, USA), at a distance of 0.50 m from both the vine trunk and the emitter.

2.2. Model identification

The model is grounded on existing flow and storage models describing the dynamic of water from soil to the atmosphere across resistances and capacitors miming an analogue electrical circuit (Calkin and Nobel, 1986). Namely, the mechanistic water flow and storage model in Calabritto et al. (2025) was adapted to be fed by two input variables and sub-models (Fig. 1). For this purpose, existing model parameters (e.g., whole soil-leaf path and storage compartment hydraulic resistances along with newly defined ones (e.g., storage capacitance, leaf area and transpiration)) were employed for model development.

Under steady-state conditions, the drop in water potential between soil and leaf conforms to the Ohm's law being proportional to driving force and hydraulic resistance across the soil-leaf path (Nobel, 2005). Hence, considering also the gravitational component, the leaf water potential (Ψ_{leaf}) is well approximated by:

$$\Psi_{leaf} = \Psi_{soil} - RT - \rho gh \quad (\text{MPa}) \tag{1}$$

where Ψ_{soil} is the soil water potential, R is the total hydraulic resistance within the whole soil-to-leaf path, T is the plant transpiration, ρ is the density of water, h is the height above the ground and g is the acceleration of gravity. The model links Ψ_{leaf} to the predicted microtensiometer signal in the trunk through the gravitational component (i.e., ρgh). The height of the microtensiometer installed in the trunk above the ground was considered for the principle of established vertical gradient of Ψ (Hellkvist et al., 1974).

According to Tyree (1988) and Cochard et al. (2002), in Eq. 1 the fluxes caused by changes in solute potential of sap are not accounted assuming the osmotic potential constant.

The water feeding T is sourced by soil through root absorption (a) aligning with the Van den Honert principle on constancy of water flow through a plant (i.e., T= a) (Nobel, 2005). However, plants can deviate from that steady-state condition because the amount of water absorbed by soil might not balance that lost via transpiration. This triggers new water flow (q) sourced by compartments apart from soil such as trunk (capacitance of the trunk) connected to the transpiration stream via the hydraulic resistance of the compartment (r) (Tyree, 1988; Nobel, 2005; Black et al., 2012). Hence, T evolves to $T = a + q$, where the term q is

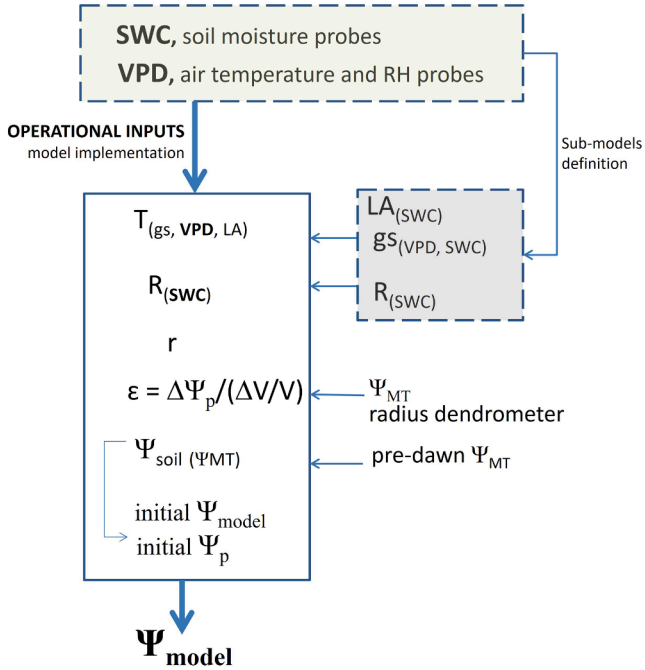

Fig. 1. Schematic flow of the model releasing estimated trunk water potential (Ψ_{model}) based on input variables (soil water content, *SWC*, vapour pressure deficit, *VPD*). Bulk elastic modulus (ε) of the storage compartment was determined via its water potential (Ψ_p) defined via microtensiometer-based trunk water potential (Ψ_{MT}) and changes in volume of the storage compartment (V). Values of V were calculated through changes in dendrometer-based stem radius. The soil water potential (Ψ_{soil}) was assumed to be equal to Ψ_{MT} measured at pre-dawn, then Ψ_{soil} was used as initial value of Ψ_{model} and Ψ_p. Hydraulic resistance of the soil-leaf path (R) and of the storage compartment (r) were retrieved from Calabritto et al. (2025). Values of R were then parametrised to soil water content, while r was maintained constant.

related to the drop of the hydrostatic gradient between xylem (Ψ_{leaf}) and the reservoir compartment (Ψ_p) according to Hunt et al. (1991). Values of *q* can be positive (T>a) or negative (T<a) accounting for the movement of water out (early morning) or in (late afternoon/night) of the compartment, respectively (Nobel, 2005). Considering that changes in time of Ψ_p depend on its elastic bulk modulus (ε) (i.e., the fractional changes in volume induced by the applied pressure $\Delta\Psi/(\Delta V/V)$) (Hunt et al., 1991; Nobel, 2005) the capacitance of a plant component (*C*) would be $C = V/\varepsilon$.

The capacitance of the leaves was not accounted in the model because it should be small compared with that of the stem (Hunt et al., 1991).

2.3. Model parameters determination

Input predictors (operational variables) of the model were *VPD* and *SWC*. These predictors were used to calibrate model parameters (R and g_s) identifying sub-models. The *r* parameter was directly retrieved from literature, while the parameters of leaf area (LA), g_s, ε, and Ψ_{soil} have been determined in this study. For details on these parameters refer to Table 1.

Soil water potential (Ψ_{soil}): the values of Ψ_{soil} were retrieved assuming that the Ψ_{trunk} at pre-dawn (when the term RT in Eq. 1 is negligible) reflects Ψ_{soil} according to Améglio et al. (1999). Hence, a sub-model estimating Ψ_{soil} was implemented by fitting Ψ_{MT} data at *VPD* < 1 kPa against the paired *SWC* over a randomly extracted train dataset (12 days, approx. 40% of the total days of the experiment). That train dataset was not used for any other model validation.

Total and compartment hydraulic resistances (R, r): the values of R

Table 1
Classification, description and source of the input variables employed for model development.

Input variables	Description	Source
Operational	*SWC*, soil water content, % vol. *VPD*, air vapor pressure deficit, kPa	Measured
Variables determined or parametrized in this study	g_s, stomatal conductance, mol m^{-2} s^{-1} fitted against *VPD* (Fig. 4) LA, vine leaf area, m^2 plant^{-1} fitted against *SWC* (Fig. 5) ε, elastic bulk modulus, MPa (Fig. 8) Ψ_{soil}, soil water potential, MPa	*Ad hoc* experiment
Calibrated parameters	R, total hydraulic resistance, MPa h kg^{-1} calibrated against *SWC* (Fig. 3)	Calabritto et al., 2025
	g_s:*VPD* model calibrated against *SWC*	Calabritto et al., 2024
Parameters from other studies	*r*, compartment hydraulic resistance, MPa h kg^{-1}	Calabritto et al., 2025

were retrieved from a closely related experiment (Calabritto et al., 2025) integrating the soil, root and trunk hydraulic resistances into a single parameter (Steppe et al., 2006). Than R values were calibrated against *SWC* (Fig. 3). The value of *r* (hydraulic resistance of the storage compartment) was directly retrieved from Calabritto et al. (2025), set at 0.01 MPa h kg^{-1} and considered constant (Hunt et al., 1991).

Vine transpiration (T): the values of T were estimated adapting the general formula of leaf transpiration (e.g., Nobel, 2005) as follow:

$$T = g_s \times \Delta P \times LA \qquad (\text{kg } H_2O \text{ h}^{-1}\text{vine}^{-1}) \tag{2}$$

where g_s is the stomatal conductance, ΔP (dimensionless) is the ratio between VPD (Pa) and atmospheric pressure (101325 Pa) (Montanaro et al., 2012), and LA (m^2) is the leaf area of the plant.

The g_s and LA values were calibrated against *VPD* and *SWC* (see below).

The nighttime transpiration rates reported in the literature are 5% - 15% of the daytime ones, though sometimes they are as high as 30% (Snyder et al., 2003; Caird et al., 2007) or even 40% (Dawson et al., 2007) of those recorded daytime. Additionally, Dayer et al. (2021) concluded that in grapevines nighttime transpiration has a negligible impact on soil water depletion. In the present study, nocturnal transpiration (from 8pm to 5am of the following day) was assumed to be 25% of the diurnal one, which is consistent with literature and available data on kiwifruit (Green et al., 1989 and references therein). In line with this, a theoretical 10% increase (or reduction) of the nighttime transpiration fraction used in the present model would translate in an increase (or reduction) of approx. 2% of the total diurnal transpiration (i.e., 0.025/1.25). This suggests that variations in nighttime water loss have a negligible impact on overall soil moisture depletion and daily water balance.

Final transpiration rate per plant (kg H_2O h^{-1}) was calculated considering that shaded leaves (60% of total leaves, see below) have higher stomatal resistance than exposed ones (Li et al., 2024) and in turn 60% of transpiration.

Vine leaf area (LA): the mean value of LA was determined using fisheye images which were processed with the Gap Light Analyzer software (Cary Institute of Ecosystem Studies, Millbrook, New York) according to Clearwater et al. (2004). To track the impact of drought, values of LA were measured in 12 vines progressively droughted and modelled (linear model) with the corresponding paired *SWC* data. Vine LA was assumed to be 40% and 60% in fully exposed and shaded leaves (Xiloyannis et al., 2000).

Stomatal conductance (gs): the g_s was estimated from *VPD* (kPa) according to Oren et al. (1999):

$$g_s = m \times \ln(VPD) + b \tag{3}$$

For this purpose, the terms *m* and b in Eq. 3 were parametrized as slope and intercept coefficients of the linear model fitting paired ln(*VPD*) and g_s measurements taken over a *VPD* range of 1.5-5 kPa in an *ad hoc* experiment using a handheld leaf porometer (LI-600; Li-Cor, USA). A minimum of four-five leaves were monitored distributed over three vines. Thereafter, g_s (Eq. 2) was achieved by converting g_s (porometer output) from mol H_2O m^{-2} s^{-1} to kg m^{-2} h^{-1} considering the molar weight of H_2O, and 3600 s h^{-1}. The model was parametrized to account for the influence of changing *SWC* within the range of 45-20% vol. on g_s, based on their relationship reported in Calabritto et al. (2024).

Storage volume (V): in the present study the storage volume was determined following the geometry described by Génard et al. (2001) considering a cylinder of 3 m total height (main trunk and permanent canes), and 0.06 m average diameter. The growth of trunk was not considered as in Calabritto et al. (2025).

Volume change of the trunk (ΔV): diurnal values of ΔV/V were determined by means of dendrometer (DR3, Ecomatik, Munich, Germany) installed in two vines per treatment (approx. 1 m above the ground) in an *ad hoc* experiment. The dendrometers measured whole-stem (i.e., over-bark) diameter variations. Hence, ΔV is the result of integrated effect of changes in the living stem tissues (bark, phloem and cambium) and the mature xylem. The change in volume of the trunk was assumed to be that of water content stored in storage compartment (Steppe et al., 2006).

Vine hydrostatic pressure gradient (ΔΨ): on the same vines equipped with dendrometers the diurnal values of ΔΨ were determined through the microtensiometer (FloraPulse, Davis, CA, USA).

2.4. Model implementation and statistics

The model and all statistics were implemented in base R (R Core Team, 2021). Simulation of Ψ_{trunk} employed a fourth-order Runge--Kutta numerical integrator with fixed step size (0.005 h). Initial values of Ψ_{trunk} in each day of simulation were posed equal to Ψ_{soil} at dawn according to Améglio et al. (1999). The period for simulation did not include the days already used for parametrization of Ψ_{soil} against *SWC* (Fig. 2).

To evaluate model stability, a sensitivity analysis was conducted by mapping model residuals (Ψ_{model} - Ψ_{MT}) across the range of the two operational input variables, *VPD* and *SWC*, using a two-dimensional surface smoothing approach (Rigden et al., 2020). All other variables were held fixed. To account for the non-uniform sample distribution across the SWC–VPD range, a locally weighted polynomial regression (LOESS) model was employed to generate a regular grid (Storlie and Helton, 2008).

The Fig. 1 summarises the model framework including the various sub-models all dependent on input variables (*SWC, VPD*) and collectively enabling the estimation of trunk water potential (Ψ_{model}).

3. Results

3.1. Sub-model parameters

The correlation between *SWC* and the Ψ_{MT} over the experimental data matching the *VPD* condition (*VPD*<1 kPa) is reported in Fig. 2. The exponential model provides a good fit to the data (Nagelkerke's pseudo R^2=0.85) and was highly significant (see Table S1).

The Fig. 3 reports the hydraulic resistance of the whole soil-leaf water path as function of *SWC* showing minimum values when soil is close to field capacity while it increases when soil dries. Variations of the predicted R and *SWC* were in good agreement (Efron's pseudo R^2=0.92).

The sub-model estimating the g_s from *VPD* data is reported in Fig. 4. The mean leaf area per vine was estimated in field and is reported in Fig. 5. Values of LAI were about 2.6 at ~40% vol. soil moisture and significantly declined with reducing *SWC* (Table S4).

3.2. Simulation of trunk water potential (Ψ_{model})

For model development, paired Ψ_{MT} and trunk diameter were measured in two vines per treatment. Diurnal changes in Ψ_{MT} showed the typical decline in the morning until the minimum (about -0.4 and -1 MPa in fully irrigated and droughted vines, respectively) was reached at about 3 p.m. (Fig. 6). Paired measurements of stem radius show the trunk shrunk during morning and recovered in the afternoon (Fig. 6). In well irrigated vines, stem radius fully recovered within the day but it remained lower than the initial one under severe (approx. -0.2 MPa pre-dawn) drought. Based on the trunk radius changes, the maximum storage volume of a vine was estimated to be approx. 2.6 ±0.07 (SE) kg

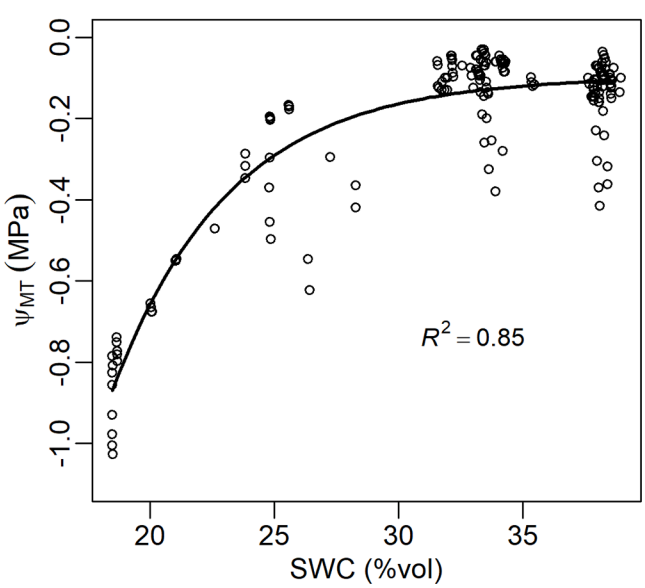

Fig. 2. Correlation between soil water content (*SWC,* % vol.) and trunk water potential (Ψ_{MT}) as measured through microtensiometer during the experiment at *VPD* values below 1 kPa. The Nagelkerke's pseudo-R^2 (Nagelkerke, 1991) was used to evaluate the goodness-of-fit of the exponential model. Details on fitting model are reported in Supplementary Table S1.

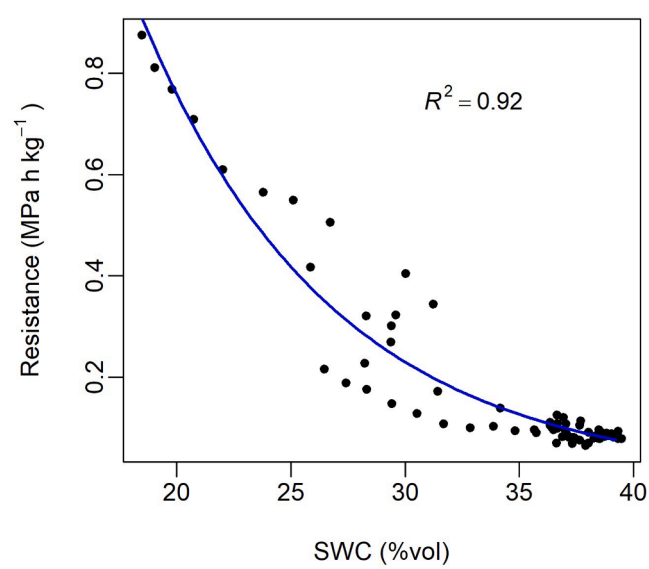

Fig. 3. Correlation between soil water content (*SWC*) and hydraulic resistance across the whole soil-leaf path. The Efron's pseudo-R^2 (Efron, 1978) was used to evaluate the goodness-of-fit of the exponential model. Details on fitting model are reported in Table S2.

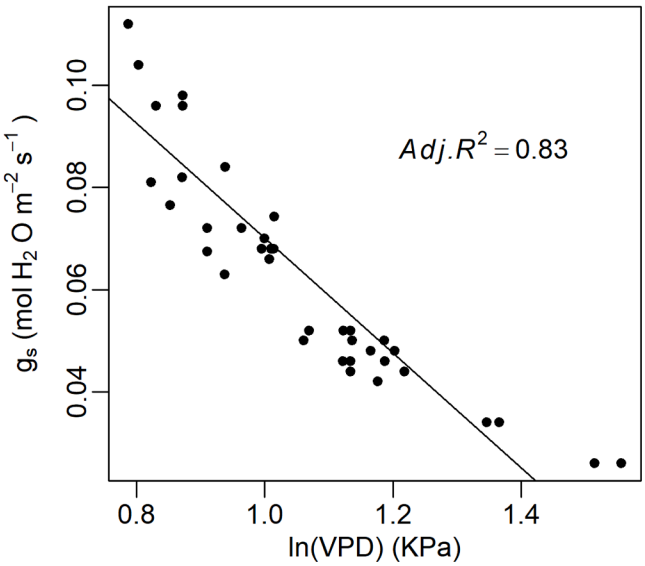

Fig. 4. Correlation between vapour pressure deficit, *VPD* (KPa, natural log scale), and stomatal conductance (g_s, mol H_2O m^{-2} s^{-1}) recorded in field grown kiwifruit vines. Details of the linear fitting model are reported in Table S3.

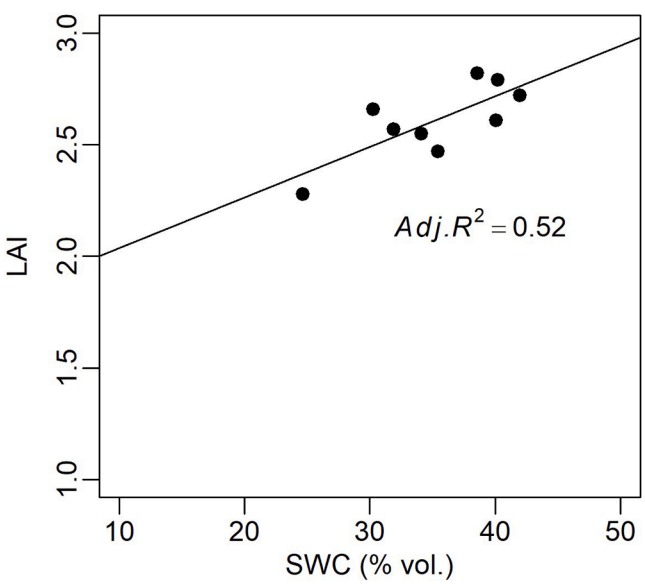

Fig. 5. Correlation between leaf area index (LAI) and soil water content (*SWC*, % vol.) recorded in field grown kiwifruit vines. Details of the linear fitting model are reported in Table S4.

water per fully irrigated and droughted vines.

The Ψ_{MT} recorded in kiwifruit was linearly related to the relative change of the compartment volume (R^2 0.97) in the 0.94-1 range of that volume independently of the irrigation treatment (Fig. 7). The slope of Ψ_{MT} versus the fractional volume change was on average 4.63 ±0.42 (SE) and 12.24 ±1.61 MPa in well-irrigated and droughted vines, respectively. Such slope values corresponded to the bulk elastic modulus (ε) and were significantly influenced by the irrigation treatment (Fig. 8). The values of ε measured during the decline of stem radius (morning-early afternoon) were comparable to those measured during the increasing radius (afternoon-evening) in both irrigation treatments (Fig. 8). These "morning-early afternoon" and "afternoon-evening" stages were identified as "OUT" and "IN", respectively when comparing ε (Fig. 8).

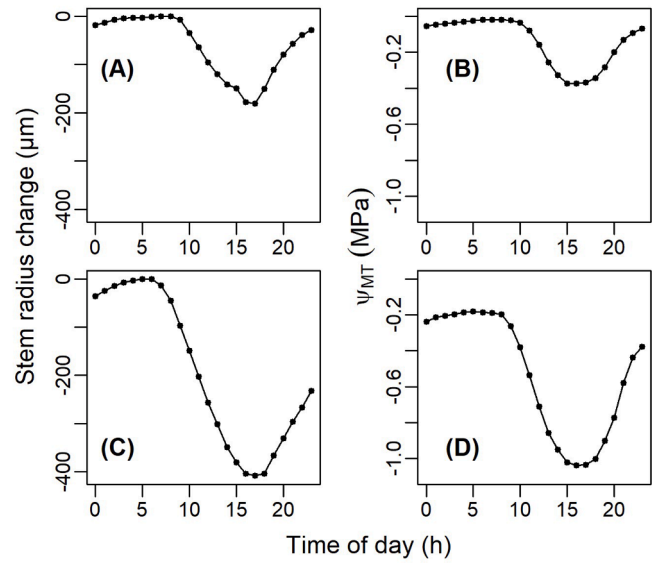

Fig. 6. Example of diurnal changes in (A, C) trunk diameter (stem radius) and (B, D) trunk water potential (Ψ_{MT}) as measured by microtensiometer. Upper row (panels A, B) refers to fully irrigated vines, bottom row (panels C, D) refers to droughted vines. Radius changes have been calculated as difference between actual values and the maximum one recorded early morning.

The water flow IN and OUT of trunk (first derivatives of the stem radius) is reported in Fig. 9. Negative values correspond to dehydration indicating the trunk contribution to the transpiration stream; in contrast positive values indicate the water flux into the storage compartment (rehydration). The dehydration/rehydration dynamic was similar in both irrigation treatments; the water flux approached the negative peak at about -0.02 and -0.035 kg h^{-1} in fully irrigated and droughted vines, respectively. By summing the daily negative values, a mean of -0.0872 ±0.008 and -0.220 ±0.021 kg day^{-1} of water transferred from the storage compartment to the transpiration stream.

The Fig. 10 shows the diurnal variations of simulated Ψ_{trunk} compared to the measured ones along with those of plant transpiration and air *VPD*. The model captured the decline and recovery pattern of the trunk pressure in fully irrigated and droughted vines during days with different maximum *VPD* namely ~ 3 kPa and ~ 5 kPa (Fig. 10A and B). Consequently, based on the transpiration dependence of Ψ_{trunk} (as per Eq. 1) the minimum values of Ψ_{trunk} were more negative in days with high maximum transpiration (~ 6.5 kg H_2O h^{-1}) (Fig. 10B) compared with days with a low transpiration peaked (~ 4 kg H_2O h^{-1}, Fig. 10A). The model simulated the diurnal Ψ_{trunk} also in vines under drought with a pre-dawn value of -0.5 MPa (Fig. 10C) or even more negative (Fig. 10D).

The sequence of the diurnal Ψ_{trunk} throughout the experiment as measured with microtensiometer and estimated with model is reported in Figs. 11 and 12. Results show that predicted Ψ_{model} values in fully irrigated vines change in sympathy with those measured by microtensiometer (Fig. 11) to the extent that (median) coefficient of determination of their linear correlation was close to 0.95 (see boxplot in Fig. 11). In droughted vines, trunk water potential starts to decline upon the treatment imposition (about one week after the start of experiment) in Ψ_{MT} and consistently in Ψ_{model}. However, during the following week, Ψ_{trunk} recovered a couple of times (see shaded period in Fig. 12B) before an uninterrupted decline was observed in the last ten days of experiment reaching approx. -1 MPa (Fig. 12). On a daily basis, the correlation between Ψ_{MT} and Ψ_{model} (excluding and including days falling in the recovery time) had a R^2 close to 0.9 (see boxplots in Figs. 12A and 12B).

Additional performance metrics were calculated for model accuracy evaluation. Namely, the mean MAE and RMSE shown in Figs. 11 and 12 increased from fully irrigated to droughted vines confirming that the

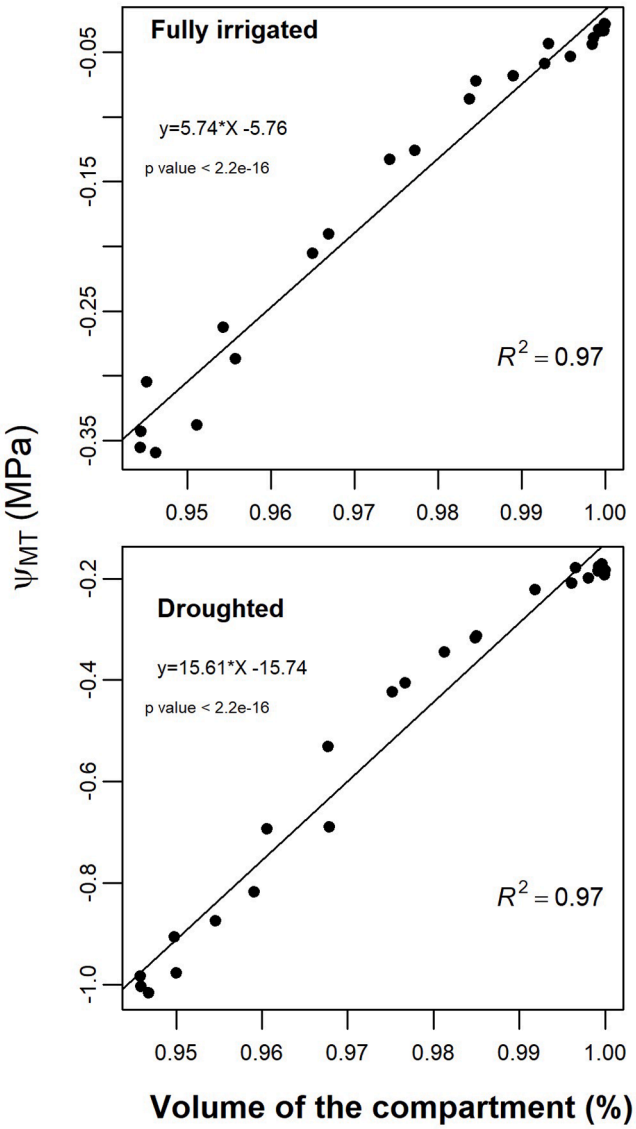

Fig. 7. Examples of correlation between diurnal values of trunk water potential measured with microtensiometer (Ψ_{MT}) and the fractional volume changes of the storage compartment measured in (top panel) fully irrigated and (bottom panel) droughted kiwifruit vines. The whole diurnal data (Fig. 6) for each treatment were pooled before fitting. The slope of the linear fitting model corresponds to the first derivatives of Ψ_{MT} and relative volume used to calculate ε.

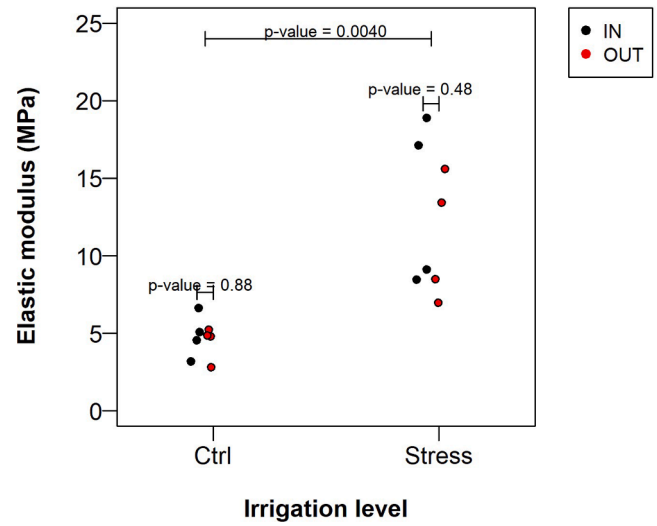

Fig. 8. Values of the bulk elastic modulus (ε) of the storage compartment determined in kiwifruit vines under full irrigation (Ctrl) and drought (Stress). The ε was separately calculated grouping the readings during the water flow IN ("afternoon-evening") and OUT ("morning-early afternoon") of the compartment. Comparisons were made by the Wilcoxon's test.

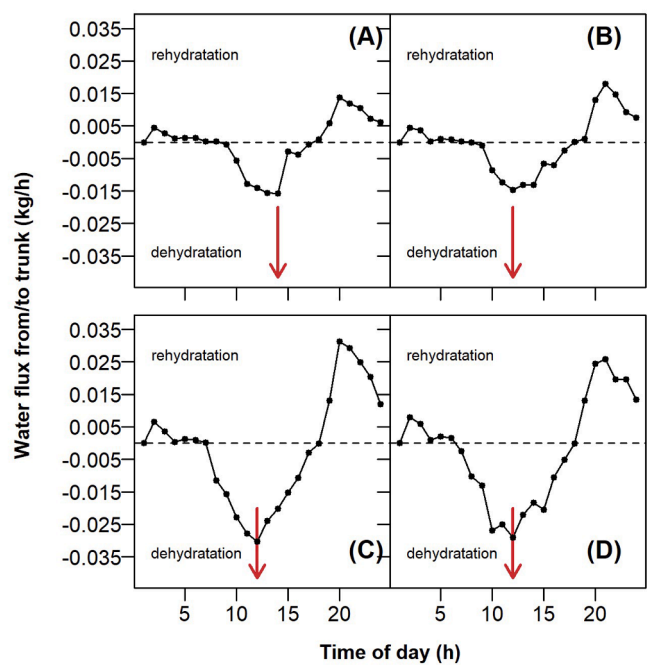

Fig. 9. Diurnal pattern of the water flux (kg h^{-1}) of the storage compartment in single vine under (A, B) full irrigation and (C, D) drought. Values are negative when water is withdrawn from the compartment and positive when the compartment is refilled. The arrows indicate the point in time when the high dehydration flux was reached.

model performs better under full irrigation. In addition, it could be noted that excluding the recovery days the MAE and RMSE improved in droughted vines, highlighting the model vulnerability during the recovery period.

Fig. 13 shows model sensitivity to changes in *SWC* and *VPD* by mapping the model residuals using a two-dimensional surface smoothing approach. In general, residuals were roughly well distributed across the range of *VPD* but model was sensitive to soil moisture deficits (Fig. 13). The model maintains an overall underestimation bias (positive residuals) in most of the examined range of *SWC*. In addition, underestimations increased when *SWC* declined below ~ 25% and *VPD* surpassed ~ 3 kPa.

In this experiment, there were a few days of recovery (see the shaded box in Fig. 12) which reduced model performance. When these days are excluded, model bias is almost entirely dependent on *SWC* at least with *SWC* above ~22% vol. (Fig. 13A). In addition, model is sensitive to *VPD* >2 kPa when *SWC* fell below that threshold.

In contrast, when these recovery days are retained in the sensitivity analysis (panel B in Fig. 13) there is an additional effect of *VPD* revealing more complex, non-linear error sensitivity. That is, although the model was stable at low *VPD* and mid-range *SWC*, the model exhibits high error sensitivity to extreme atmospheric dryness (*VPD* > 3 kPa and *SWC* < 25% vol.).

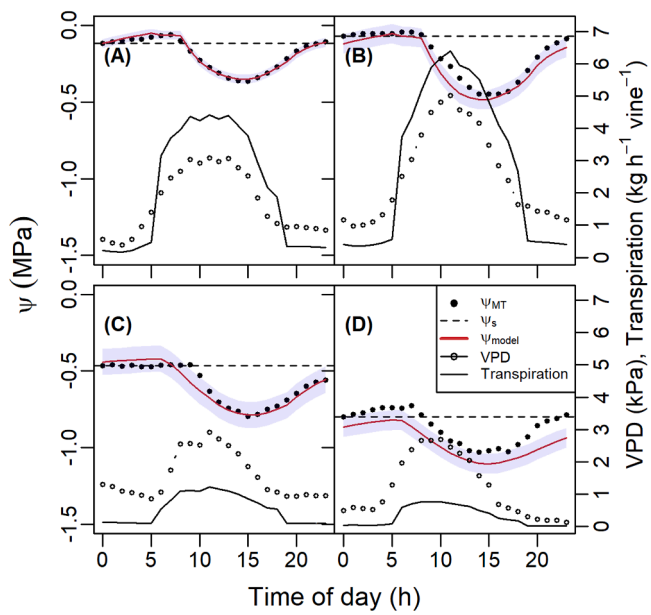

Fig. 10. Examples of diurnal oscillation in trunk water potential recorded by microtensiometer (Ψ_{MT}) and modelled (Ψ_{model}), and of vapour pressure deficit (*VPD*) and transpiration. The horizontal dashed line indicates the soil water potential (Ψ_{soil}) assumed constant during the day. The shaded areas indicate the 95% prediction interval of the model.

4. Discussion

The primary purpose of the present study was to model the diurnal trunk water potential (Ψ_{trunk}) using only two measured input variables, namely soil water content (*SWC*) and atmospheric vapour pressure deficit (*VPD*). Estimated trunk water potential (Ψ_{model}) was compared with that measured *in vivo* by means of microtensiometers installed in vines under full irrigation or progressively droughted. The resulting Ψ_{model} values were closely related to those in actual ones showing a median R^2 up to approx. 0.95.

The main advantage of the model proposed is the limited number (two) of operational inputs variables. Results would support the employment of a combination of *model & sensor* to enable easy, large scale and relatively low-cost monitoring of plant water status and in turn irrigation management.

4.1. Soil water potential, hydraulic resistance and transpiration sub-models

The ambition to use a low number of input variables was necessarily supported by sub-models, where additional parameters were defined from known or specifically developed relationships, or calibrated. These inputs were the hydraulic resistances of the whole soil-leaf path (R) and of the storage compartment (*r*), plant leaf area and transpiration (T). The soil water potential (Ψ_{soil}) was also estimated, as it represents a key input in modelling the hydrostatic potential gradient between the soil and the leaves (or trunk).

Estimation of Ψ_{soil} values assumed the correspondence of soil water potential to trunk water potential measured pre-dawn when sap flow would be negligible (Améglio et al., 1999). This assumption might be criticised in case of nocturnal transpiration. That is, Caird et al. (2007) propose that nighttime transpiration could generate "*soil-plant predawn water potential disequilibrium*" possibly reducing accuracy of estimation of soil moisture availability based on pre-dawn plant water potential measurement. Although a specific evaluation of the impact of nighttime transpiration on Ψ_{leaf} and Ψ_{soil} equilibrium would be desirable, plant water potential measured pre-dawn remains a solid proxy of Ψ_{soil} (Zeng et al., 2025). As expected, soil drying significantly affected the estimated Ψ_{soil} particularly when *SWC* drop below about 30% indicating that the observed decrease in Ψ_{soil} was effectively captured by the non-linear function (Fig. 2, Table S1). Although Ψ_{soil} might be considered variable on a diurnal basis (Calabritto et al., 2025), in this study, for model simplification Ψ_{soil} was assumed constant because of its relatively narrow oscillation (approx. 1-4% of the initial value, in well irrigated (Dichio unpublished data)).

Even though soil moisture can be highly heterogeneous, variations of *SWC* close to the trunk, as in this study and in those of García-Tejero et al. (2017) and Calabritto et al. (2025), are much more directly related to vine water uptake. Hence, they were pertinent to model development as they provided information on how Ψ_{trunk} changed with changing *SWC*. However, future applied work might account for soil moisture far from the trunk, as in Autovino et al. (2018), to further improve model scalability.

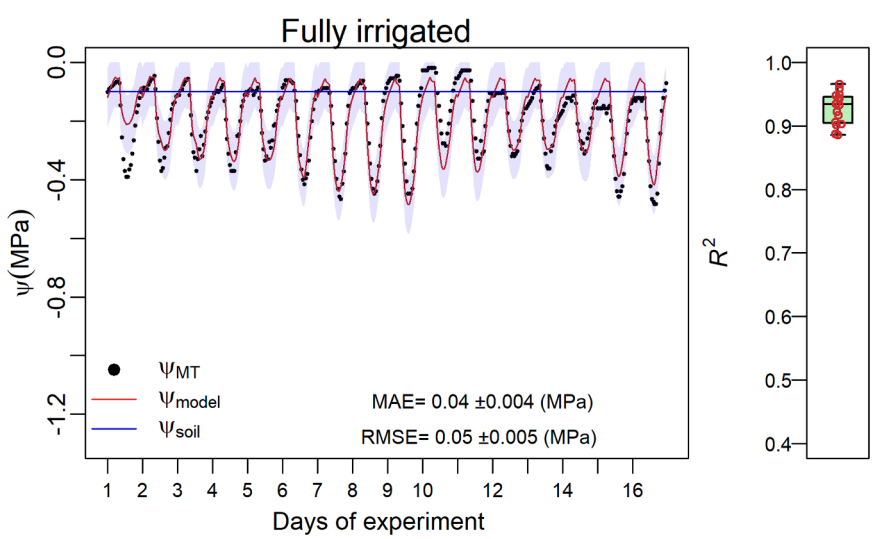

Fig. 11. Sequential diurnal oscillations of trunk water potential measured by means of microtensiometer (Ψ_{MT}) and estimated (Ψ_{model}), and soil water potential (Ψ_{soil}) in fully irrigated field-grown vines. Next to the panel, a boxplot of the coefficient of determination calculated from the linear fit between measured Ψ_{MT} and Ψ_{model} for each day. Data are the mean of two vines. The shaded area indicates the prediction interval (95%) of the model. Please note that data of the present figure have not been used for parametrization of functions.

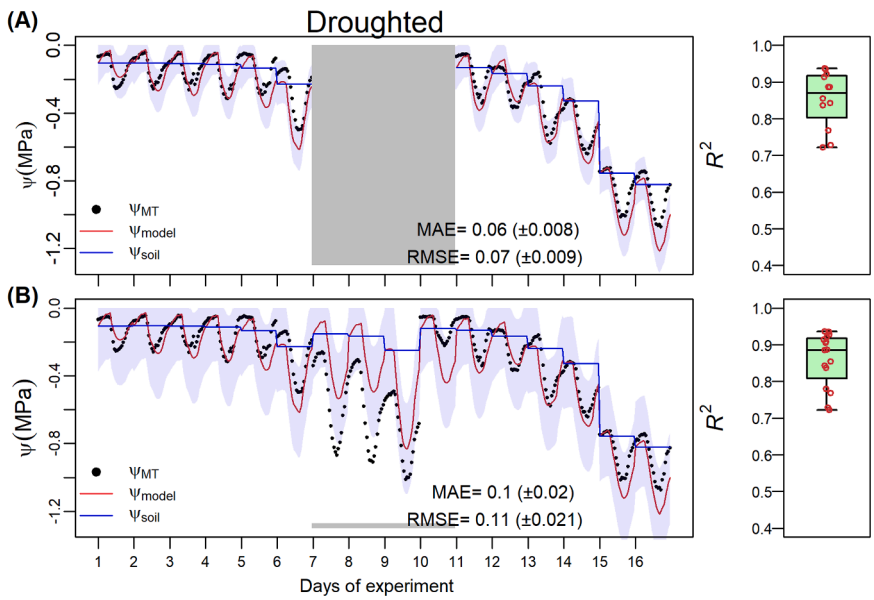

Fig. 12. Sequential diurnal oscillations of trunk water potential measured by means of microtensiometer (Ψ_{MT}) and estimated (Ψ_{model}), and soil water potential (Ψ_{soil}) in progressively droughted field-grown vines. The shaded area around the model line indicates the prediction interval (95%) of the model. In panel (A) the days belonging to a recovery period (dark box) were not considered for model bias determination and R^2 calculation, in (B) all the days were used. Note that the upper bound of the prediction interval is clipped at a maximum of 0 MPa and that data have not previously been used for parametrization of functions.

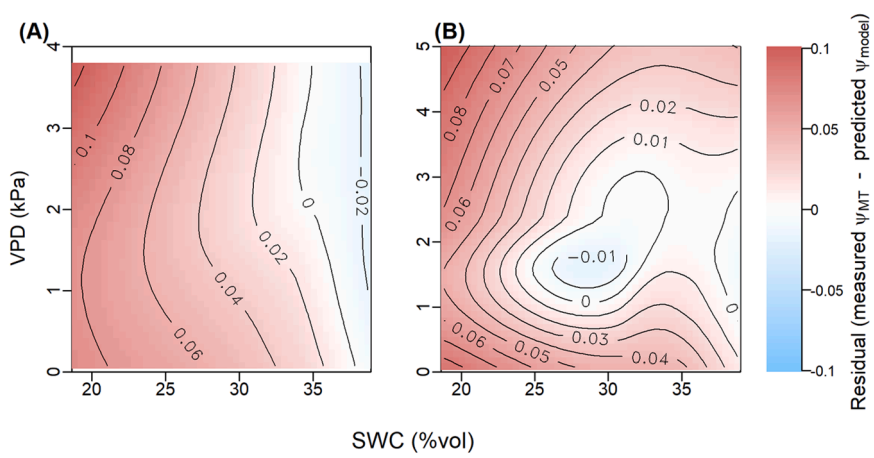

Fig. 13. Sensitivity analysis of model residuals across the two operational input variables (soil water content (*SWC*) and vapor pressure deficit (*VPD*)) recorded during the experimental period, (A) excluding and (B) including rewatering days (see shaded area in Fig. 12).

The sub-model estimating R in response to soil drying shows that declining *SWC* induced a significant exponential increase in R (Fig. 3) in line with existing results in grapevine and oak (Baert et al., 2015). Hence, it was essential to introduce in the model *SWC*-dependent values of R. In contrast with this, the resistance of the storage compartment was considered constant as in other researches (Hunt et al., 1991; Calabritto et al., 2025).

A key parameter of the model was the transpiration (T) acting as the driver of plant water movement which is often associated to the current in electrical circuit contributing to set the hydrostatic pressure gradient between leaf and the below parts of the soil-plant continuum (Calkin and Nobel, 1986; Hunt et al., 1991). For the estimate of T (Eq. 2), values of instantaneous g_s were retrieved via *ad hoc* experiment parametrizing g_s as function of natural log of *VPD* (Fig. 4). Although several models of g_s have been proposed (Gao et al., 2002; Buckley et al., 2003), such a method is widely employed in research (e.g., Cunningham, 2004; Grossiord et al., 2020) and is based on a consistent relationship between g_s at low *VPD* identifying a reference g_s corresponding to that at 1 kPa (Oren et al., 1999). The resulting g_s linear sub-model (Table S3) is consistent with the general sensitivity of g_s to *VPD* (i.e., slope equals to approx. 0.6 × intercept) (Grossiord et al., 2020). Based on the dependence of leaf and stem hydraulics on stomatal sensitivity to *VPD* (Brodribb and Jordan, 2008) the significant parametrization of g_s achieved would have contributed to a solid estimation of T and in turn of Ψ_{model}. Values of estimated T (not shown) were consistent with those of sap flow measurements of a closely related experiment (Calabritto et al., 2025). This finding highlights that whole-plant canopy transpiration data are advisable to validate estimates of T ensuring realistic plant hydraulics model.

4.2. Hydraulic features and modelling trunk water potential

The core operating principle of the present model was rooted in the analogy of water movement with the electrical circuit. That is, water moves from soil to atmosphere across a series of resistances in response to gradients in water potential (Nobel, 2005 and references therein). The

model has been developed accounting for water sourced from a capacitor (trunk tissue) different than soil helping to cope with time lag between changing transpiration (as driven by *VPD*) and leaf/trunk water potential in trees (Oliva Carrasco et al., 2015). In a previous attempt to model Ψ_{trunk} as response variable of *VPD* and *SWC* (Di Biase et al., 2025), the Ψ_{MT} series were shifted backward by 4 hours to account for that time lag and improve the model fitting. A similar approach was employed in other studies. For instance, Pagay (2022) and Wan et al. (2023) modelled Ψ_{trunk} in grapevine and +50 forestry tree species, respectively, artificially aligned time course of *VPD* and Ψ_{trunk} values. Hence, integrating the capacitor in a non-steady-state model would contribute to expand current knowledge in applied modelling plant water relations.

In this study, the storage compartment volume was approx. 60% lower than that calculated in a field grown droughted kiwifruit (Nuzzo et al., 1997) experiencing a similar drop in water potential from pre-dawn to midday (~ 0.7-0.8 MPa). Such an apparent discrepancy might be explained by considering the putative differences in trunk size, which likely influenced the storage compartment volume (Génard et al., 2001; Salomón et al., 2017). That is, the number of plants per hectare was 1,000 in the present study, whereas it was 500 in Nuzzo et al. (1997). The volume changes in the storage compartment have been assumed equal to those in water volume (Steppe et al., 2006). The total daily negative flux values determined in the present study (Fig. 9) represented the water released to the transpiration stream and was significantly influenced by the irrigation treatment. Namely, the water released by a droughted vine was significantly ($p < 0.05$, Wilcox's test) 2.5 times greater than that in well irrigated. That amount of water was in the magnitude of that released by *Quercus ilex* trees with a comparable trunk diameter (Salomón et al., 2017). However, considering the daily irrigation volumes (up to 60 m^3 ha^{-1} day^{-1}) and those released by the compartment (up to 0.22 m^3 ha^{-1}), it appears that the typology of kiwifruit orchard examined would be almost entirely dependent on root water uptake which is challenging for irrigation management.

The hydrostatic pressure causing the fractional change of the volume of the capacitor is captured by the bulk elastic modulus (ε) which determines the shrinkage of the stem (Dietrich et al., 2018). Incidentally, the shrinkage in droughted vines had larger magnitude compared to that in fully irrigated vines confirming trunk tissue sourced more water (as discussed above). Elastic modulus may vary among different stem tissues (Scholz et al., 2007). Several studies have reported that most diameter fluctuations occur in the elastic living tissues of the bark and that only minor or no contractions are observed in the mature xylem (Zweifel et al., 2000; Steppe, 2004). These findings suggest that xylem is a more rigid material (i.e., has a lower elasticity) (Scholz et al., 2008). In the present study, diurnal changes in trunk radius were employed to determine values of ε under the assumption that stem radius changes occur mainly in the elastic tissue of the bark whereas the woody parts of the stem undergo only small diurnal fluctuations (Zweifel and Hasler, 2001). In addition, the procedure for ε estimation is consistent with that in other studies (Genard et al., 2001; Steppe and Lemeur, 2007). Although species might differ in elastic properties of the tissues involved in shrinkage (Heine 1971, Steppe and Lemeur, 2007), ε observed were in the magnitude of those reported in saplings of *P. radiata* breeds (De Diego et al., 2013) and in crop herbs (Bartlett et al., 2012). Under drought conditions, an increase in leaf ε has been associated to increasing drought (Bartlett et al., 2012). In line with this, in the present study ε increased by approx. three times under water limitation compared to values in fully irrigated vines (Fig. 8). The response of Ψ_{trunk} to change in the fractional volume of the compartment (Fig. 7) was linear within the early ~ 10% volume reductions in both fully irrigated and droughted vines. Such a linearity fits with those in Calkin and Nobel (1986) and Hunt and Nobel (1987) and with the general idea that the "*initial slope of a pressure-volume curve is approximately constant over a range of relative water content from 0.95 to 0.80*" (Hunt et al., 1991).

Over the range of Ψ_{MT} values observed in this study, linear model fitting the changes of hydrostatic pressure per unit change in relative volume had different slope. This might be explained accounting for the changes in ε after drought-induced soil drying (Fig. 8). The functional dependency of ε on drought-induced change in fractional volume of tissue might be nonlinear as reported in forest tree species and olive (Roberts et al., 1981; Dichio et al., 2003). Although the minimum Ψ_{trunk} measured in the present study indicate severe water stress (Di Biase et al., 2025), more efforts are required to establish the type of dependency (e.g., linear or curvilinear) of ε on *SWC* in kiwifruit covering as wide as possible range of Ψ.

The model had a good fitting based on the R^2 calculated from daily correlation between Ψ_{MT} and Ψ_{model} in both irrigation treatments. However, additional accuracy metrics are advisable as discussed in Montanaro et al. (2023). For example, although the use of MAE would be encouraged as it is less sensitive to outliers, both the scale-dependent RMSE and MAE metrics were significantly lower ($p < 0.05$, Wilcox's test) in fully irrigated vines compared to droughted ones. Additionally, these performance metrics increased when the recovery period (shaded area in Fig. 12) was included in the analysis. This envisages some model limitations when drought alternates to recovery. That is, the model sensitivity analysis confirmed that including a few days of recovery reduced the model's performance, showing high error sensitivity to extreme atmospheric dryness and soil moisture deficit. Hence, the sensitivity analysis reveals that more efforts are required to reduce model vulnerability under high *VPD* and rewatering conditions.

The satisfactorily fitting between Ψ_{MT} and Ψ_{model} was likely attributable to the model ability to reproduce the lag existing between transpiration and Ψ_{trunk} peaks (Calkin and Nobel, 1986; Di Biase et al., 2025) (Fig. 10). This result is difficult to discuss because of limited dynamic Ψ_{trunk} models developed in kiwifruit. In addition, often only the *VPD* was considered as explanatory variable of Ψ_{trunk} under stable and non-limiting soil moisture (Blanco and Kalcsits, 2023). In Di Biase et al. (2025), based on a correlative linear approach (i.e., $\Psi_{trunk} \sim SWC$) it was proposed to introduce *SWC* as a non-linear term to putatively further improve the explanation of Ψ_{trunk} dependencies. In the present model, the impact of *SWC* has been considered within sub-models implementation adopting the resulting non-linear dependency of g_s, leaf area and soil-plant hydraulic resistance (see sub-model in Tables S1 and S2). Hence, in the present study, rather than a correlative approach a mechanistic one has been used to account for the influence of *SWC* on Ψ_{trunk} contributing to the progress of model development in this specific field.

5. Limitations

The model did not account for the changing water relations existing during the recovering stage following a drought exposure. According to M&M section, drought vines were initially recovered to avoid an abrupt stress occurrence. This likely influenced the poor alignment of Ψ_{model} and Ψ_{MT} observed during recovery in vine under progressive drought (see shaded days Fig. 12), significantly reducing model performance. This can be explained considering that g_s might be uncoupled by *SWC* during recovering because of "stomatal inertia" possibly due to accumulation of drought-related signals (McAdam, 2023). Hence, modelling the recovery stage requires further efforts before the model can be widely applicable for irrigation management. Moreover, application of this model under extreme atmospheric conditions (e.g., very high *VPD*) would require recalibration of g_s to collect the proper model coefficients, avoiding unrealistic g_s values.

This study was developed when vines had completely developed LAI limiting its application during the early stage of growing season when leaf area develops (Xiloyannis et al., 2000). Values of ε were defined at control and severe drought conditions with Ψ_{trunk} ranging from about -0.05 to about -1 MPa (Fig. 7). While estimating ε more frequently during the progression of drought would likely further tailor the model to *SWC* variations. The capacitance of the leaves was not accounted in the present model because it should be small compared with that of the

stem (Hunt et al., 1991), and because it would not be influential on Ψ_{MT} readings due to the topography of foliage compared to that of the insertion point of the microtensiometer. However, this remains to be specifically tested in a model focusing kiwifruit species.

The developed trunk water potential model has been tailored on kiwifruit with specific parameters (R, *r*, g_s) limiting its transferability to other tree species which likely differ in the above mentioned parameters.

6. Conclusions

This paper presents an effective dynamic model of Ψ_{trunk} based on two operational input variables, *VPD* and *SWC*, which captures the time lag between changing transpiration and trunk water potential in kiwifruit. Results would promote a wide deployment of plant-based sensors such as microtensiometer to be used as benchmark of Ψ_{trunk} values considering its relationship with variable *SWC* or *VPD* conditions. The model is promising for future development of a vine water relations tool even though its parametrization under recovery days, specific environmental and cropping conditions (e.g., rootstocks, cultivars, and canopy structures) would be required.

Funding

This study has been supported by the Ecosistema TECH4YOU – Technologies for climate change adaptation and quality of life improvement—Missione 4 Componente 2 Investimento 1.5 NextGenerationEU ECS00000009 CUPC43 C22000400006—PP 3.3.1 SMART WATER.

CRediT authorship contribution statement

Giuseppe Montanaro: Writing – review & editing, Writing – original draft, Visualization, Supervision, Resources, Investigation, Formal analysis, Data curation, Conceptualization. **Maria Calabritto:** Writing – review & editing, Writing – original draft, Formal analysis, Data curation. **Alba Nicoletta Mininni:** Writing – review & editing, Supervision, Resources, Formal analysis, Data curation. **Bartolomeo Dichio:** Writing – review & editing, Supervision, Resources, Funding acquisition, Conceptualization.

Declaration of competing interest

The authors declare that they have no known competing financial interests or personal relationships that could have appeared to influence the work reported in this paper.

Acknowledgements

We are grateful to Roberto Di Biase and Rocco Sarli for their support in data collection from microtensiometer and dendrometer installed in the kiwifruit orchard. This study was part of the initiatives of Phen-Italy, the Italian node of the European Infrastructure for multi-scale Plant Phenomics and Simulation for Food Security in a Changing Climate EMPHASIS.

Supplementary materials

Supplementary material associated with this article can be found, in the online version, at doi:10.1016/j.scienta.2026.115219.

Data availability

Data will be made available on request.

References

Ali, A., Hussain, T., Zahid, A., 2025. Smart irrigation technologies and prospects for enhancing water use efficiency for sustainable agriculture. AgriEngineering 7 (4), 106. https://doi.org/10.3390/agriengineering7040106.

Améglio, T., Archer, P., Cohen, M., Valancogne, C., Daudet, F.A., Dayau, S., Cruiziat, P., 1999. Significance and limits in the use of predawn leaf water potential for tree irrigation. Plant Soil 207, 155–167. https://doi.org/10.1023/A:1026415302759.

Autovino, D., Rallo, G., Provenzano, G., 2018. Predicting soil and plant water status dynamic in olive orchards under different irrigation systems with Hydrus-2D: Model performance and scenario analysis. Agric. Water Manag. 203, 225–235. https://doi.org/10.1016/j.agwat.2018.03.015.

Baert, A., De Schepper, V., Steppe, K., 2015. Variable hydraulic resistances and their impact on plant drought response modelling. Tree Physiol. 35 (4), 439–449. https://doi.org/10.1093/treephys/tpu078.

Bartlett, M.K., Scoffoni, C., Sack, L., 2012. The determinants of leaf turgor loss point and prediction of drought tolerance of species and biomes: a global meta-analysis. Ecol. Lett. 15 (5), 393–405. https://doi.org/10.1111/j.1461-0248.2012.01751.x.

Black, M., Patterson, K., Gould, K., Clearwater, M., 2012. Physiological responses of kiwifruit vines (*Actinidia chinensis* Planch. Var. *Chinensis*) to trunk girdling and root pruning. New Zeal J. Crop Hort. 40 (1), 31–41. https://doi.org/10.1080/01140671.2011.603343.

Blanco, V., Kalcsits, L., 2021. Microtensiometers accurately measure stem water potential in woody perennials. Plants 10 (12), 2780. https://doi.org/10.3390/plants10122780.

Blanco, V., Kalcsits, L., 2023. Long-term validation of continuous measurements of trunk water potential and trunk diameter indicate different diurnal patterns for pear under water limitations. Agric. Water Manag. 281, 108257. https://doi.org/10.1016/j.agwat.2023.108257.

Brodribb, T.J., Jordan, G.J., 2008. Internal coordination between hydraulics and stomatal control in leaves. Plant Cell Env. 31 (11), 1557–1564. https://doi.org/10.1111/j.1365-3040.2008.01865.x.

Buckley, T.N., Mott, K.A., Farquhar, G.D., 2003. A hydromechanical and biochemical model of stomatal conductance. Plant Cell Env. 26 (10), 1767–1785. https://doi.org/10.1046/j.1365-3040.2003.01094.x.

Caird, M.A., Richards, J.H., Donovan, L.A., 2007. Nighttime Stomatal Conductance and Transpiration in C3 and C4 Plants. Plant Physiol. 143 (1), 4. https://doi.org/10.1104/pp.106.092940.

Calabritto, M., Mininni, A.N., De Pauw, D.J., Green, S., Dichio, B., Steppe, K., 2025. Combining plant-based sensing and mechanistic modelling to quantify hydraulic resistance and capacitance for real-time irrigation in Mediterranean yellow-fleshed kiwifruit orchards. Agric. Water Manag. 316, 109607. https://doi.org/10.1016/j.agwat.2025.109607.

Calabritto, M., Mininni, A.N., Di Biase, R., Pietrafesa, A., Dichio, B., 2024. Spatio-temporal dynamics of root water uptake and identification of soil moisture thresholds for precision irrigation in a Mediterranean yellow-fleshed kiwifruit orchard. Front. Plant Sci. 15, 1472093. https://doi.org/10.3389/fpls.2024.1472093.

Calkin, H.W., Nobel, P.S., 1986. Nonsteady-state analysis of water flow and capacitance for Agave deserti. Canad. J. Bot. 64 (11), 2556–2560. https://doi.org/10.1139/b86-338.

Carella, A., Massenti, R., Marra, F.P., Catania, P., Roma, E., Lo Bianco, R., 2024. Combining proximal and remote sensing to assess 'Calatina' olive water status. Front. Plant Sci. 15, 1448656. https://doi.org/10.3389/fpls.2024.1448656.

Clearwater, M.J., Lowe, R.G., Hofstee, B.J., Barclay, C., Mandemaker, A.J., Blattmann, P., 2004. Hydraulic conductance and rootstock effects in grafted vines of kiwifruit. J. Exp. Bot. 55 (401), 1371–1382. https://doi.org/10.1093/jxb/erh137.

Cochard, H., Coll, L., Le Roux, X., Améglio, T., 2002. Unraveling the effects of plant hydraulics on stomatal closure during water stress in walnut. Plant Physiol 128 (1), 282–290. https://doi.org/10.1104/pp.010400.

Cunningham, S., 2004. Stomatal sensitivity to vapour pressure deficit of temperate and tropical evergreen rainforest trees of Australia. Trees 18, 399–407. https://doi.org/10.1007/s00468-004-0318-y.

Dawson, T.E., Burgess, S.S.O., Tu, K.P., Oliveira, R.S., Santiago, L.S., Fisher, J.B., Simonin, K.A., Ambrose, A.R., 2007. Nighttime transpiration in woody plants from contrasting ecosystems. Tree Physiol 27 (4), 561–575. https://doi.org/10.1093/treephys/27.4.561.

Dayer, S., Herrera, J.C., Dai, Z., Burlett, R., Lamarque, L.J., Delzon, S., Bortolami, G., Cochard, H., Gambetta, G.A., 2021. Nighttime transpiration represents a negligible part of water loss and does not increase the risk of water stress in grapevine. Plant Cell Env. 44 (2), 387–398. https://doi.org/10.1111/pce.13923.

De Diego, N., Sampedro, M.C., Barrio, R.J., Saiz-Fernandez, I., Moncalean, P., Lacuesta, M., 2013. Solute accumulation and elastic modulus changes in six radiata pine breeds exposed to drought. Tree Physiol. 33 (1), 69–80. https://doi.org/10.1093/treephys/tps125.

Di Biase, R., Calabritto, M., Mininni, A.N., Montanaro, G., Dichio, B., 2025. Microtensiometer-based trunk water potential as a plant water status indicator in kiwifruit under different soil water availability. Irrig Sci 43, 937–954. https://doi.org/10.1007/s00271-025-01020-1.

Dichio, B., Xiloyannis, C., Angelopoulos, K., Nuzzo, V., Bufo, S.A., Celano, G., 2003. Drought-induced variations of water relations parameters in *Olea europaea*. Plant Soil 257, 381–389. https://doi.org/10.1023/A:1027392831483.

Dietrich, L., Zweifel, R., Kahmen, A., 2018. Daily stem diameter variations can predict the canopy water status of mature temperate trees. Tree Physiol 38 (7), 941–952. https://doi.org/10.1093/treephys/tpy023.

Efron, B., 1978. Regression and ANOVA with Confident-Nonconfident Data. Biometrika 65 (1), 113–121. https://doi.org/10.1093/biomet/65.1.113.

Fereres, E., Goldhamer, D., 2003. Suitability of stem diameter variations and water potential as indicators for irrigation scheduling of almond trees. J. Hortic. Sci. Biotech. 78 (2), 139–144. https://doi.org/10.1080/14620316.2003.11511596.
Fernández, J.E., 2014. Plant-based sensing to monitor water stress: Applicability to commercial orchards. Agric. Water Manag. 142, 99–109. https://doi.org/10.1016/j.agwat.2014.04.017.
Gao, Q., Zhao, P., Zeng, X., Cai, X., Shen, W., 2002. A model of stomatal conductance to quantify the relationship between leaf transpiration, microclimate and soil water stress. Plant Cell Env. 25, 1373–1381. https://doi.org/10.1046/j.1365-3040.2002.00926.x.
García-Tejero, I.F., Hernández, A., Padilla-Díaz, C.M., Díaz-Espejo, A., Fernández, J.E., 2017. Assessing plant water status in a hedgerow olive orchard from thermography at plant level. Agric Water Manag 188, 50–60. https://doi.org/10.1016/j.agwat.2017.04.004.
Génard, M., Fishman, S., Vercambre, G., Huguet, J.-G., Bussi, C., Besset, J., Habib, R., 2001. A Biophysical Analysis of Stem and Root Diameter Variations in Woody Plants. Plant Physiol 126 (1), 188–202. https://doi.org/10.1104/pp.126.1.188.
Girona, J., Marsal, J., Arbones, A., Dejong, T.M., 2004. A comparison of the combined effect of water stress and crop load on fruit growth during different phenological stages in young peach trees. J. Hortic. Sci. Biotech. 79 (2), 308–315. https://doi.org/10.1080/14620316.2004.11511766.
Goudriaan, J., van Laar, H.H., 1994. Modelling Potential Crop Growth Processes. Kluwer Academic Publ., Dordrecht – Boston – London https://doi.org/10.1007/978-94-011-0750-1. –.
Green, S., Clothier, B., Jardine, B., 2003. Theory and practical application of heat pulse to measure sap flow. Agron. J. 95 (6), 1371–1379. https://doi.org/10.2134/agronj2003.1371.
Green, S.R., McNaughton, K.G., Clothier, B.E., 1989. Observations of night-time water use in kiwifruit vines and apple trees. Agric. Meteorol. 48 (3-4), 251–261. https://doi.org/10.1016/0168-1923(89)90072-5.
Grossiord, C., Buckley, T.N., Cernusak, L.A., Novick, K.A., Poulter, B., Siegwolf, R.T.W., Sperry, J.S., McDowell, N.G., 2020. Plant responses to rising vapor pressure deficit. New Phytol 226 (6). https://doi.org/10.1111/nph.16485. Article 6.
Haberstroh, S., Scarpa, F., Seeger, S., Christen, A., Werner, C., 2025. Continuous Stem Water Potential Measurements of a Diffuse-Porous Tree Species Offer New Insights Into Tree Water Relations. Ecohydrology 18 (1), e2761. https://doi.org/10.1002/eco.2761.
Heine, R.W., 1971. Hydraulic conductivity in trees. J Exp. Bot. 22, 503–511. https://doi.org/10.1093/jxb/22.3.503.
Hellkvist, J., Richards, G., Jarvis, P.G., 1974. Vertical gradients of water potential and tissue water relations in Sitka spruce trees measured with the pressure chamber. J. Appl. Ecol. 637–667. https://doi.org/10.2307/2402215.
Hunt, E.R., Nobel, P.S., 1987. Non-steady-state water flow for three desert perennials with different capacitances. Aust. J. Plant Physiol. 14 (4), 363–375. https://doi.org/10.1071/PP9870363.
Hunt, E.R., Running, S.W., Federer, C.A., 1991. Extrapolating plant water flow resistances and capacitances to regional scales. Agric. Meteorol. 54 (2–4), 169–195. https://doi.org/10.1016/0168-1923(91)90005-B.
Jones, H.G., 2004. Irrigation scheduling: Advantages and pitfalls of plant-based methods. J Exp. Bot. 55 (407), 2427–2436. https://doi.org/10.1093/jxb/erh213.
Li, Z., Zhao, L., Zhao, Z., Cai, H., Xing, L., Cui, N., 2024. Estimating the transpiration of kiwifruit using an optimized canopy resistance model based on the synthesis of sunlit and shaded leaves. Agric. Water Manag. 306, 109193. https://doi.org/10.1016/j.agwat.2024.109193.
Marsal, J., Girona, J., 1997. Relationship between leaf water potential and gas exchange activity at different phenological stages and fruit loads in peach trees. J Am. Soc. Hort. Sci. 122 (3), 415–421. https://doi.org/10.21273/JASHS.122.3.415.
McAdam, S.A.M., 2023. What stops stomata reopening after a drought? Tree Physiol 43 (6), 879–882. https://doi.org/10.1093/treephys/tpad031.
McCutchan, H., Shackel, K.A., 1992. Stem-water potential as a sensitive indicator of water stress in prune trees (*Prunus domestica* L. cv. French). J Am. Soc. Hort. Sci. 117 (4), 607–611.
Meinzer, F.C., 2003. Functional convergence in plant responses to the environment. Oecologia 134 (1), 1–11. https://doi.org/10.1007/s00442-002-1088-0.
Meinzer, F.C., James, S.A., Goldstein, G., 2004. Dynamics of transpiration, sap flow and use of stored water in tropical forest canopy trees. Tree Physiol 24 (8), 901–909. https://doi.org/10.1093/treephys/24.8.901.
Meinzer, F.C., Johnson, D.M., Lachenbruch, B., McCulloh, K.A., Woodruff, D.R., 2009. Xylem hydraulic safety margins in woody plants: coordination of stomatal control of xylem tension with hydraulic capacitance. Funct. Ecol. 23, 922–930. https://doi.org/10.1111/j.1365-2435.2009.01577.x.
Montanaro, G., Dichio, B., Xiloyannis, C., Lang, A., 2012. Fruit transpiration in kiwifruit: environmental drivers and predictive model. AoB Plan. https://doi.org/10.1093/aobpla/pls036 pls036.
Montanaro, G., Petrozza, A., Rustioni, L., Cellini, F., Nuzzo, V., 2023. Phenotyping key fruit quality traits in olive using rgb images and back propagation neural networks. Plant Phenomics 5, 0061. https://doi.org/10.34133/plantphenomics.0061.
Nagelkerke, N.J.D., 1991. A note on a general definition of the coefficient of determination. Biometrika 78 (3), 691–692. https://doi.org/10.1093/biomet/78.3.691.
Naor, A., 1998. Relations between leaf and stem water potentials and stomatal conductance in three field-grown woody species. J. Hortic. Sci. Biotech. 73 (4), 431–436. https://doi.org/10.1080/14620316.1998.11510995.
Nobel, P.S., 2005. Physiochemical and Environmental Plant Physiology, 3rd ed. Elsevier Academic Press, Burlington.
Noun, G., Lo Cascio, M., Spano, D., Marras, S., Sirca, C., 2022. Plant-based methodologies and approaches for estimating plant water status of Mediterranean tree species: a semi-systematic review. Agronomy 12 (9), 2127. https://doi.org/10.3390/agronomy12092127.
Nuzzo, V., Dichio, B., Xiloyannis, C., Piccotino, D., Massai, R., 1997. Contribution to transpiration of different tissues of kiwifruit vines from their water reserves. Acta Hortic. 444, 329–334. https://doi.org/10.17660/ActaHortic.1997.444.51.
Oliva Carrasco, L., Bucci, S.J., Di Francescantonio, D., Lezcano, O.A., Campanello, P.I., Scholz, F.G., Rodriguez, S., Madanes, N., Cristiano, P.M., Hao, G.Y., Holbrook, N.M., Goldstein, G., 2015. Water storage dynamics in the main stem of subtropical tree species differing in wood density, growth rate and life history traits. Tree Physiol 35 (4), 354–365. https://doi.org/10.1093/treephys/tpu087.
Oren, R., Sperry, J.S., Katul, G.G., Pataki, D.E., Ewers, B.E., Phillips, N., Schäfer, K.V.R., 1999. Survey and synthesis of intra- and interspecific variation in stomatal sensitivity to vapour pressure deficit. Plant Cell Env. 22 (12), 1515–1526. https://doi.org/10.1046/j.1365-3040.1999.00513.x.
Pagay, V., 2022. Evaluating a novel microtensiometer for continuous trunk water potential measurements in field-grown irrigated grapevines. Irrig. Sci. 40 (1), 45–54. https://doi.org/10.1007/s00271-021-00758-8.
Park, H., Han, J., Myoung, S., Kim, M., Lim, H., Kim, D., Lee, G., 2025. Non-invasive wearable sensors for monitoring plant health. Macromol. Res. 1–12. https://doi.org/10.1007/s13233-025-00384-9.
Parra-López, C., Abdallah, S.B., Garcia-Garcia, G., Hassoun, A., Trollman, H., Jagtap, S., Gupta, S., Aït-Kaddour, A., Makmuang, S., Carmona-Torres, C., 2025. Digital technologies for water use and management in agriculture: Recent applications and future outlook. Agric. Water Manag. 309, 109347. https://doi.org/10.1016/j.agwat.2025.109347.
Paschalis, A., De Kauwe, M.G., Sabot, M., Fatichi, S., 2024. When do plant hydraulics matter in terrestrial biosphere modelling? Glob Chang Biol 30 (1), e17022. https://doi.org/10.1111/gcb.17022.
R Core Team, 2021. R: A language and environment for statistical computing. https://www.R-project.org/.
Restrepo-Acevedo, A.M., Guo, J., Novick, K., Humphrey, V., Zweifel, R., Konings, A.G., Koch, G., Knowles, J., Anderegg, L.D.L., Peters, J.M.R., Paligi, S., Schenk, H.J., Beverly, D., Magh, R.K., Yao, Y., Hackmann, C.A., Bohrer, G., Browne, M., Carminati, A., Kannenberg, S.A., 2026. Continuous monitoring of plant water potential: sensor-based approaches and best practices. New Phytol 251 (1), 569–588. https://doi.org/10.1111/nph.71194.
Rigden, A.J., Mueller, N.D., Holbrook, N.M., Pillai, N., Huybers, P., 2020. Combined influence of soil moisture and atmospheric evaporative demand is important for accurately predicting US maize yields. Nat. Food 1 (2), 127–133. https://doi.org/10.1038/s43016-020-0028-7.
Roberts, S.W., Strain, B.R., Knoerr, K.R., 1981. Seasonal variation of leaf tissue elasticity in four forest tree species. Physiol. Plant. 52 (2), 245–250. https://doi.org/10.1111/j.1399-3054.1981.tb08500.x.
Salomón, R.L., Limousin, J.M., Ourcival, J.M., Rodríguez-Calcerrada, J., Steppe, K., 2017. Stem hydraulic capacitance decreases with drought stress: Implications for modelling tree hydraulics in the Mediterranean oak *Quercus ilex*. Plant Cell Env. 40 (8), 1379–1391. https://doi.org/10.1111/pce.12928.
Scalisi, A., Bresilla, K., Grilo, F.S., 2017. Continuous determination of fruit tree water-status by plant-based sensors. Italus Hortus 24 (2), 39–50. https://doi.org/10.26353/j.itahort/2017.2.3950.
Scharwies, J.D., Dinneny, J.R., 2019. Water transport, perception, and response in plants. J Plant Res 132 (3), 311–324. https://doi.org/10.1007/s10265-019-01089-8.
Scholz, F.C., Bucci, S.J., Goldstein, G., Meinzer, F.C., Franco, A.C., Miralles-Wilhelm, F., 2008. Temporal dynamics of stem expansion and contraction in savanna trees: withdrawal and recharge of stored water. Tree Physiol 28, 469–480. https://doi.org/10.1093/treephys/28.3.469.
Scholz, F.G., Bucci, S.J., Goldstein, G., Meinzer, F.C., Franco, A.C., Miralles-Wilhelm, F., 2007. Biophysical properties and functional significance of stem water storage tissues in Neotropical savanna trees. Plant Cell Env. 30 (2), 236–248. https://doi.org/10.1111/j.1365-3040.2006.01623.x.
Scholz, F.G., Phillips, N.G., Bucci, S.J., Meinzer, F.C., Goldstein, G., 2011. Hydraulic capacitance: biophysics and functional significance of internal water sources in relation to tree size. In: Meinzer, F.C., Lachenbruch, B., Dawson, T.E. (Eds.), Size-and Age-Related Changes in Tree Structure and Function. Springer Science & Business Media, Netherlands. https://doi.org/10.1007/978-94-007-1242-3_13.
Shackel, K., 2011. A plant-based approach to deficit irrigation in trees and vines. HortScience 46 (2), 173–177. https://doi.org/10.21273/HORTSCI.46.2.173.
Snyder, K.A., Richards, J.H., Donovan, L.A., 2003. Night-time conductance in C3 and C4 species: Do plants lose water at night? J Exp Bot 54 (383), 861–865. https://doi.org/10.1093/jxb/erg082.
Steppe, K., 2004. Diurnal dynamics of water flow through trees: design and validation of a mathematical flow and storage model. Ghent University, Ghent. Ph.D. Thesis.
Steppe, K., De Pauw, D.J.W., Lemeur, R., Vanrolleghem, P.A., 2006. A mathematical model linking tree sap flow dynamics to daily stem diameter fluctuations and radial stem growth. Tree Physiol 26 (3), 257–273. https://doi.org/10.1093/treephys/26.3.257.
Steppe, K., Lemeur, R., 2007. Effects of ring-porous and diffuse-porous stem wood anatomy on the hydraulic parameters used in a water flow and storage model. Tree Physiol 27 (1), 43–52. https://doi.org/10.1093/treephys/27.1.43.
Storlie, C.B., Helton, J.C., 2008. Multiple predictor smoothing methods for sensitivity analysis: Description of techniques. Reliab. Eng. Syst. Saf. 93 (1), 28–54. https://doi.org/10.1016/j.ress.2006.10.012.

Tyree, M.T., 1988. A dynamic model for water flow in a single tree: evidence that models must account for hydraulic architecture. Tree Physiol 4 (3), 195–217. https://doi.org/10.1093/treephys/4.3.195.

Vaccaro, G., Fusco, M., Alagna, V., Franco, L., Motisi, A., Iovino, M., 2025. Assessing microtensiometers for monitoring stem water potential in mandarin (*Citrus reticulata* Blanco) orchard under different irrigation regimes. Agric. Water Manag. 320, 109873. https://doi.org/10.1016/j.agwat.2025.109873.

Van den Honert, T.H., 1948. Water transport in plants as a catenary process. Discuss Faraday Soc. 3, 146–153. https://doi.org/10.1039/DF9480300146.

Velazquez-Chavez, L.J., Daccache, A., Mohamed, A.Z., Centritto, M., 2024. Plant-based and remote sensing for water status monitoring of orchard crops: Systematic review and meta-analysis. Agric. Water Manag. 303, 109051. https://doi.org/10.1016/j.agwat.2024.109051.

Villalobos, F.J., Testi, L., García-Tejera, O., López-Bernal, Á., Tejado, I., Vinagre, B.M., 2025. Measuring the Diurnal Variation of Root Conductance in Olive Trees Using Microtensiometers and Sap Flow Sensors. Plant Soil 509 (1), 999–1012. https://doi.org/10.1007/s11104-024-06873-7.

Walsh, J.J., Mangina, E., Negrão, S., 2024. Advancements in imaging sensors and AI for plant stress detection: a systematic literature review. Plant Phenomics 6, 0153. https://doi.org/10.34133/plantphenomics.0153.

Wan, L., Zhang, Q., Cheng, L., Liu, Y., Qin, S., Xu, J., Wang, Y., 2023. What determines the time lags of sap flux with solar radiation and vapor pressure deficit? Agric Meteorol 333, 109414. https://doi.org/10.1016/j.agrformet.2023.109414.

Wu, N., Xu, J., Ren, L., Song, W., 2025. Application and perspectives of plant flexible sensors in precision agriculture: material, fabrication and functional analysis. Comput. Electron. Agric. 239, 110991. https://doi.org/10.1016/j.compag.2025.110991.

Wu, S., Li, Y., Wang, Q., Cai, Y., Teng, P., Li, W., Zhang, F., Xu, L.P., Wang, S., 2025. Wearable plant sensing devices for health monitoring. Wearable Electron. 2, 100–115. https://doi.org/10.1016/j.wees.2025.03.002.

Xiloyannis, C., Nuzzo, V., Dichio, B., Celano, G., Montanaro, G., 2000. Characterization of training system in relation to water use efficiency in apricot and kiwifruit plants. Acta Hortic. 537, 207–213. https://doi.org/10.17660/ActaHortic.2000.537.21.

Zeng, Y., Verhoef, A., Vereecken, H., Ben-Dor, E., Veldkamp, T., Shaw, L., Van Der Ploeg, M., Wang, Y., Su, Z., 2025. Monitoring and modeling the soil-plant system toward understanding soil health. Rev. Geophys. 63. https://doi.org/10.1029/2024RG000836 e2024RG000836.

Zweifel, R., Häsler, R., 2001. Dynamics of water storage in mature subalpine *Picea abies*: temporal and spatial patterns of change in stem radius. Tree Physiol. 21 (9), 561–569. https://doi.org/10.1093/treephys/21.9.561.

Zweifel, R., Item, H., Häsler, R., 2000. Stem radius changes and their relation to stored water in stems of young Norway spruce trees. Trees 15 (1), 50–57. https://doi.org/10.1007/s004680000072.